

Orientation workspace of a parallel manipulator with a fixed point

J-P Merlet

INRIA Sophia-Antipolis, BP 93, 06902 Sophia-Antipolis Cedex, France
E-mail: merlet@caphorn.inria.fr

Abstract—We consider a parallel manipulator for which we want to determine the possible rotation around a fixed point. We present an algorithm enabling to calculate all the possible motions on the unit sphere of the extremity of any unit vector linked to the mobile platform. This algorithm enables to take into account the constraints on the links lengths, mechanical limits on the joints and interference between the links.

I. INTRODUCTION

Determining the workspace of a manipulator is an important step in the design phase. For the serial link manipulator family called "wrist-partionned" one can represent independently the translations of the wrist and the rotation of the end-effector around this center. For a parallel manipulator as the one represented in figure 1 the constraints limiting the workspace are: limited range of the linear actuators, mechanical limits on the passive joints and link interference. This kind of constraints imply that the reachable region for a point of the end-effector is deeply dependent upon the current orientation of the end-effector. Therefore the workspace is completely imbedded in $R^3 \times SO(3)$ and there is no graphical method to display it in human readable form.

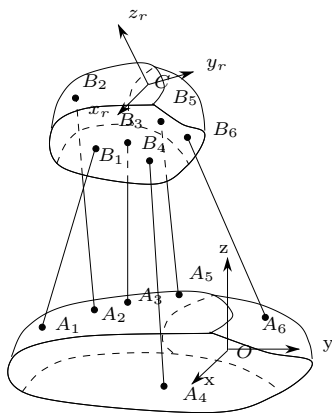


Figure 1: A parallel manipulator: two plates are connected through 6 articulated links whose length can be modified through a jack.

Therefore in most of the works addressing the workspace

problem only some subset of the full workspace is calculated. For example it is usual to compute the reachable region of a point of the end-effector in a given plane and for a given orientation of the end-effector. In most of the works the possible translations in this plane are determined by using a discretisation method (at each point of a grid the constraint are calculated and the extremal points define the border of the workspace). The constraints taken into account are mostly the limitation on the links lengths [4] and sometimes the mechanical limits of the joints [3, 9, 13]. This method is time consuming and may yield to incorrect results as there may be void into the workspace. Another approach uses the fact that on the border of the workspace the velocity in the direction of the outer normal of the border is equal to zero [1, 8, 12] but it is not clear how to take into account the mechanical limits on the passive joints and possible link interference.

A better method has been proposed by Gosselin who present a fast geometrical method enabling to find the border of the workspace according to the links lengths constraints either in the 2D case [5] or in the 3D case [6]. We have proposed an extension of this method [10] which enable to take into account also the mechanical limits on the joints and the link interference. Some results have been presented for the orientation workspace of parallel manipulators, mainly for planar manipulators, but these works deal only with the limitation on the link lengths [7, 11].

We present here an algorithm which enable to represent the possible rotation of the end-effector around a given point under the assumption that this point is fixed in the reference frame.

II. ORIENTATION WORKSPACE

We will suppose that point C (origin of the frame linked to the end-effector, see figure 1) is fixed. Let \mathbf{N} be a segment of length 1 attached to the end-effector with origin C. As the end-effector rotates around C the extremity N_e of \mathbf{N} moves on the unit sphere centered in C. We will represent the motion of N_e for any rotation of the end-effector around a fixed vector \mathbf{X}_1 followed by a rotation around another fixed vector \mathbf{X}_2 . For example we may represent the motion of the normal to the end-effector for any rotation around the vectors of the reference frame \mathbf{x}, \mathbf{z} (figure 2). This kind of representation enables to represent two rotational degree of freedom of the robot.

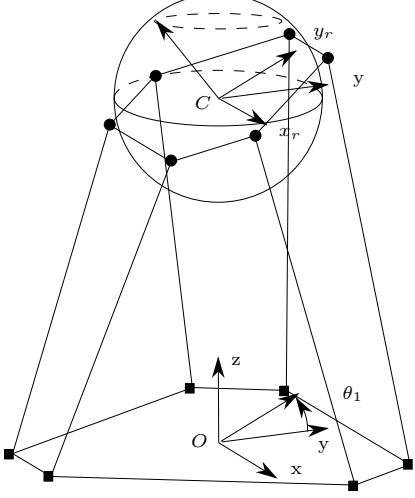


Figure 2: An example of the representation of the orientation workspace: we will represent the motion on the unit sphere of the normal z_r of the end-effector for a given rotation around the x axis of angle θ_1 when the end-effector rotates around the z axis (the motion is the ellipsis in dashed line). Here $\mathbf{X}_1 = [1, 0, 0]$, $\mathbf{X}_2 = [0, 0, 1]$.

A. Possible motion of the points B_i

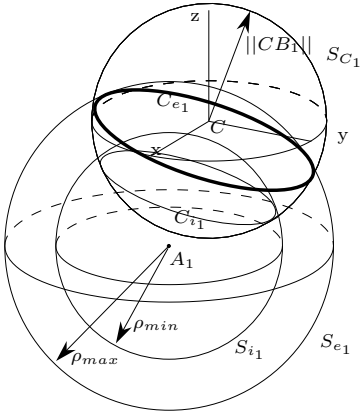


Figure 3: Point B_i must lie on the sphere S_{C_i} centered in C with radius $\|CB_i\|$ and between the sphere S_{e_i}, S_{i_i} centered in A_i whose radii are ρ_{min}, ρ_{max}

We first examine the possible motion of a point B_i , center of the joint of link i on the end-effector under the assumption that the only constraints are that the length ρ of the link $A_i B_i$ must lie in the range ρ_{min}, ρ_{max} . Firstly let us notice that point B_i rotate around C and therefore must lie on a sphere S_{C_i} whose center is C and whose radius is the constant norm of the vector \mathbf{CB}_i . According to the link length constraints point B_i must also lie inside a volume defined by the spheres S_{e_i}, S_{i_i} centered in A_i whose radii are ρ_{min}, ρ_{max} (figure 3).

Therefore the allowable zone Z_{B_i} for a point B_i on S_{C_i}

S_{C_i} with the spheres S_{e_i}, S_{i_i} . For a given rotation around \mathbf{X}_1 as the end-effector rotates around \mathbf{X}_2 point B_i will move on a circle C_{B_i} (figure 4).

First let us suppose that there is no intersection between C_{B_i} and C_{e_i}, C_{i_i} . In that case either B_i can be allowed to lie on the whole circle C_{B_i} (case 1 on the figure) or C_{B_i} is fully outside the zone Z_{B_i} (case 2) and therefore for any position of B_i on C_{B_i} (and consequently for any rotation of the end-effector) the link length will always be greater than ρ_{max} or lower than ρ_{min} . In order to find in which

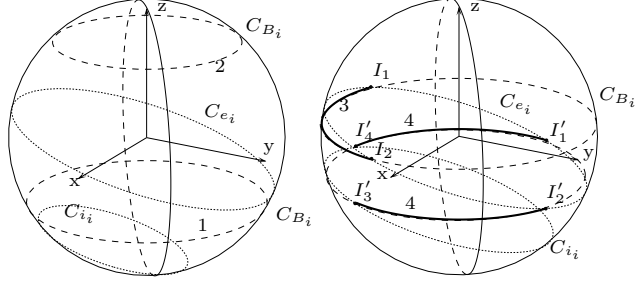


Figure 4: For a given rotation around \mathbf{X}_1 point B_i moves on a circle C_{B_i} (in dashed line) as the end-effector rotates around \mathbf{X}_2 . If C_{B_i} lie fully inside the zone delimited by C_{e_i}, C_{i_i} (represented in fine dashed line) the whole circle is allowed for B_i (1). At the opposite if C_{B_i} is fully outside this zone (2) no rotation is allowed for B_i .

case we are it is sufficient to test any position of B_i on C_{B_i} (for a given position of B_i the end-effector position and orientation is fully known). If for this particular point the link length satisfy the constraint then any position on the whole circle will be allowed.

Let us assume now that there are intersection points between C_{B_i} and C_{e_i} or C_{i_i} . Except in some particular cases there will be either two intersection points I_1, I_2 (C_{B_i} intersect only one of the circles, see 3 on figure 4) or four intersection points $I'_{1..4}$ (case 4 on figure 4). These intersection points define arcs of circle on C_{B_i} . On these arcs either the link length is outside its allowed range for any point on the arc or the link length constraints are always satisfied and the arc describe valid positions of B_i (theses arcs will be called the *valid arcs*). Therefore to determine the valid arcs it is sufficient to test the link length for one particular point of each arc (for example the middle point). After completing this test we have determined the possible positions of B_i on C_{B_i} for a given rotation around \mathbf{X}_1 as a list of arcs of circle.

B. Calculation of the allowable zone for \mathbf{N}

Let us suppose that point B_i moves on one of its valid arcs on C_{B_i} , A_j^i . As \mathbf{N} is attached to the end-effector the point N_e , extremity of \mathbf{N} , will also move on an arc of circle ${}^N A_j^i$ lying in a plane parallel to the plane containing C_{B_i} . Let suppose that the location of B_i is one of the extremal points of A_j^i . For this position of B_i the orientation

corresponding rotation matrix. We have:

$$\mathbf{N} = \mathbf{C}\mathbf{N}_e = \mathbf{C}\mathbf{B}_i + \mathbf{B}_i\mathbf{N}_e \quad (1)$$

Let $\mathbf{C}\mathbf{N}_e^r$ be the known coordinates vector of N_e expressed in the relative frame and $\mathbf{C}\mathbf{B}_i^r$ the coordinates vectors of B_i in the relative frame. We have:

$$\mathbf{B}_i\mathbf{N}_e = R_e\mathbf{C}\mathbf{N}_e^r - R_e\mathbf{C}\mathbf{B}_i^r \quad (2)$$

Combining equations (1) and (2) we get:

$$\mathbf{N} = \mathbf{C}\mathbf{B}_i + R_e(\mathbf{C}\mathbf{N}_e^r - \mathbf{C}\mathbf{B}_i^r) \quad (3)$$

Equation (3) enables to find the location of the extremal points of ${}^N A_j^i$ according to the location of the extremal points of A_j^i .

Now we have to determine the radius and center coordinates of ${}^N A_j^i$. Let $\mathbf{C}\mathbf{N}_e^1$ be the the vector obtained from $\mathbf{C}\mathbf{N}_e^r$ after rotation around \mathbf{X}_1 . The radius ${}^N r_j^i$ of ${}^N A_j^i$ is given by $\|\mathbf{X}_2 \times \mathbf{C}\mathbf{N}_e^1\|$ where $\|\cdot\|$ denotes the Euclidian norm and \times the cross-product, and its center ${}^N C_j^i$ may be determined by $\mathbf{C}^N \mathbf{C}_j^i = (\mathbf{X}_2 \cdot \mathbf{C}\mathbf{N}_e^1) \mathbf{X}_2$. Therefore the valid arcs of circle described by N_e are fully determined as soon as the arcs of circle A_j^i are known. On these arcs the constraints on link i are satisfied. The center and radius of the arcs ${}^N A_j^i$ is identical for every link. Therefore in order to find the motion of N_e on the unit sphere we have simply to find the intersection of the set of arcs ${}^N A_j^i$ for i varying from 1 to 6. By calculating this intersection for a set of angles of rotation around \mathbf{X}_1 we are able to determine an approximation of the possible locations of N_e on the whole unit sphere. Note that the range on the variation of the angle of rotation should not be greater than π in order to avoid any interference between the various sections. We need therefore to show two unit spheres to illustrate the orientation motion for a 2π rotation around \mathbf{X}_1 . We show on figure 5 the result for the manipulator defined in [2].

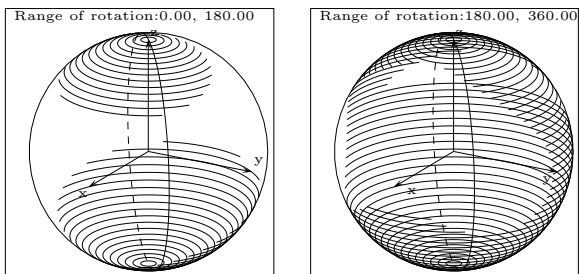


Figure 5: The possible motion of the normal of the end-effector on the unit sphere for a first rotation around the x-axis of angle in the range $[0-2\pi]$ followed by a rotation around the z-axis

III. MECHANICAL LIMITS ON THE JOINTS

We may modelize the mechanical limits on a joint in the same manner as in [10]: we assume that the operator may

that the segment $A_i B_i$ will lie inside the pyramid if the joints angle are within the mechanical limits of the joint. For example in figure 6 the pyramid has four faces (this will be a good model in the case where the joint is below the base and the link go through a square opening). For a

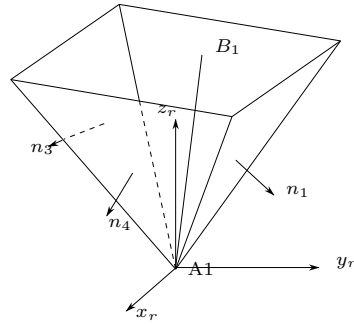


Figure 6: A model for the constraint on the joint A_1 .

given circle C_{B_i} let us consider its intersection points with the circle C_{e_i}, C_{i_i} together with its intersection points with the various faces of the pyramids. All these points define arc of circles which are either fully valid or fully invalid. To find the valid arcs we consider the middle point of each arc and test if in this position of B_i the links lengths are within the range and if B_i lie inside the pyramid. The allowable position of B_i are the arcs where these conditions are fulfilled (figure 7). From the allowable arcs for each

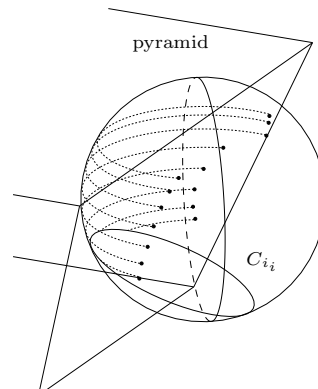


Figure 7: The intersection points of the circles C_{B_i} with the pyramid and with C_{e_i}, C_{i_i} (dotted points) enable to define the allowable arc for B_i (in dashed line)

B_i we deduce the allowable arcs for \mathbf{N} as in the previous section (figure 8).

IV. DEALING WITH LINKS INTERFERENCE

Clearly during a rotation motion links interference may occur. We assume that the links are cylindrical with radius r_i and that there will be interference between link i, j if the distance between them is less than $r_i + r_j$. Let us

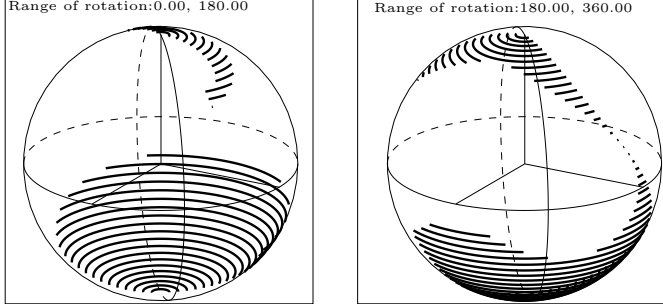


Figure 8: The possible motion of the normal of the end-effector on the unit sphere for a first rotation around the x-axis of angle in the range $[0-2\pi]$ followed by a rotation around the z-axis. The constraints on the links lengths and the mechanical limits on the joint in A_i have been taken into account.

remember [10] that the distance between two links is either the distance d_{ij} between the line if the points of their common perpendicular lie on the links or the minimum distance between the points A_i, A_j, B_i, B_j . We will denote by $d(A, B)$ the distance between points A, B . Let us consider that point B_i moves on a circle C_{B_i} i.e. that the angle of rotation around \mathbf{X}_1 is fixed. As B_i moves on C_{B_i} the angle of rotation θ_2 around \mathbf{X}_2 vary from 0 to 2π . For two links i, j we consider the various cases where there is links interference. We thus write:

$$d_{ij} = r_i + r_j \quad d(A_i, A_j) = r_i + r_j \quad (4)$$

$$d(A_i, B_j) = r_i + r_j \quad d(B_i, B_j) = r_i + r_j \quad (5)$$

$$d(B_i, A_j) = r_i + r_j \quad (6)$$

These equations can be written as functions of θ_2 and have all the same form :

$$a_1 \sin(\theta_2) + a_2 \cos(\theta_2) + a_3 = 0 \quad (7)$$

which yield to two solutions in θ_2 . Therefore on a circle C_{B_i} we may have up to 10 position of B_i such that the distance between the links i and j is $r_i + r_j$ (figure 9). These points define arcs on C_{B_i} and on these arcs either the distance between the links is lower than $r_i + r_j$ (which means that we have links interference) or greater than this quantity (no links interference).

Therefore we can describe now the general procedure enabling to determine the valid arcs for B_i on a given C_{B_i} . On this C_{B_i} we consider the various transition points i.e. the intersection points of C_{B_i} with C_{e_i}, C_{i_i} , the intersection points of C_{B_i} with the pyramids faces and the points on C_{B_i} where the distance between the link i and another link j is $r_i + r_j$. These points define arcs of circle on C_{B_i} and the valid arcs for B_i are the arcs where the middle point verify all the constraints. From the set of valid arcs for B_i we deduce the valid arcs for \mathbf{N} as presented in section II. B.

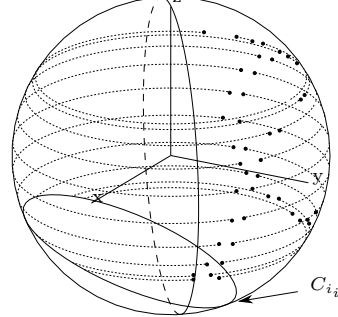


Figure 9: On some point of the circles C_{B_i} (in dashed line) the distance between the link i and another link j is equal to $r_i + r_j$ (dotted point)

V. EXAMPLES

We show in figures 10, 11 the possible location of the extremity of the normal of the end-effector for successive rotation around \mathbf{x}, \mathbf{z} for the manipulator described in [2]. In each case we consider that we have constraints on the link lengths, mechanical limits on the joints and we check for link interference (the radii of the links is 2cm).

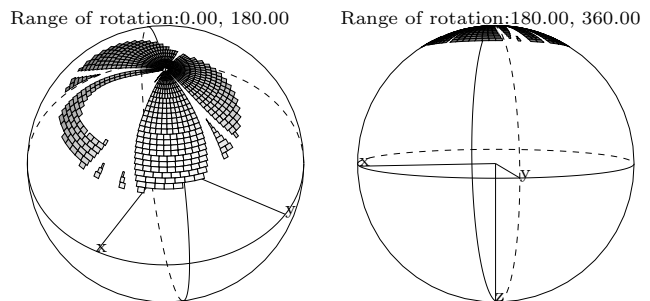


Figure 10: In gray possible location of the normal to the end-effector for the location of C defined by $x_C = y_C = 0, z_C = 530$.

VI. CONCLUSION

We have presented in this paper an algorithm to find the orientation workspace of a parallel manipulator. This algorithm shows the possible motion on the unit sphere of an axis linked to the mobile plate. It takes into account all the constraints limiting the workspace of a parallel manipulator: maximum and minimum of the links lengths, mechanical limits on the joints and checks links interference. We intend to use this algorithm to study motion planning of parallel manipulators.

VII. *

References

- [1] Agrawal S.K. Workspace boundaries of in-parallel manipulator systems. In *ICAR*, pages 1147–1152, Pise, June 19-22, 1991.

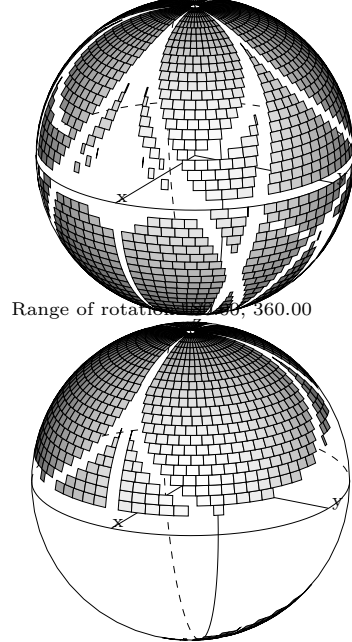


Figure 11: In gray possible location of the normal to the end-effector for the location of C defined by $x_C = y_C = 0, z_C = 600$.

[2] Arai T., Cleary K., and others . Design, analysis and construction of a prototype parallel link manipulator. In *IEEE Int. Workshop on Intelligent Robots and Systems*, July 3-6, 1990.

[3] Cleary K. and Arai T. A prototype parallel manipulator: kinematics construction, software, workspace results and singularity analysis. In *IEEE Int. Conf. on Robotics and Automation*, pages 566–571, Sacramento, April 11-14, 1991.

[4] Fichter E.F. A Stewart platform based manipulator: general theory and practical construction. *The Int. J. of Robotics Research*, 5(2):157–181, 1986.

[5] Gosselin C. Determination of the workspace of 6-dof parallel manipulators. *Trans. of the ASME, J. of Mechanisms Transmissions and Automation in Design*, 1989.

[6] Gosselin C., Lavoie E., and Toutant P. An efficient algorithm for the graphical representation of the three-dimensional workspace of parallel manipulators. In *ASME Mechanisms Conf.*, Phoenix, September , 1992.

[7] Jo D.Y. and Haug E.J. Workspace analysis of closed loop mechanisms with unilateral constraints. In *ASME Design Automation Conf.*, pages 53–60, Montréal, May , 1989.

[8] Landsberger S.E. and Shanmugasundram A.P. Workspace of parallel link crane. In *IMACS/SICE*

turing Systems, pages 479–486, Kobe, September 16-20, 1992.

[9] Lee K-M and Shah D.K. Kinematic analysis of a three-degrees-of-freedom in-parallel actuated manipulator. *IEEE J. of Robotics and Automation*, 4(3):354–360, June , 1988.

[10] Merlet J-P. Manipulateurs parallèles, 5eme partie : Détermination de l'espace de travail à orientation constante. Research Report 1645, INRIA, March , 1992.

[11] Pennock G.R. and Kassner D.J. The workspace of a general geometry planar three degree of freedom platform manipulator. *ASME Journal of Mechanical Design*, 115:269–276, June , 1993.

[12] Weng T-C., Sandor G.N., and Xu Y. On the workspace of closed-loop manipulators with ground mounted rotary-linear actuators and finite size platform. In *ASME Design and Automation Conf.*, pages 55–61, Boston, September 27-30, 1987.

[13] Yang D.C.H. and Lee T.W. Feasibility study of a platform type of robotic manipulator from a kinematic viewpoint. *Trans. of the ASME, J. of Mechanisms Transmissions and Automation in design*, 106:191–198, June , 1984.